Plant Physiology®

Plant Physiology, 2025, **199**, kiaf361
https://doi.org/10.1093/plphys/kiaf361
Advance access publication 18 August 2025
Research Article

The reduced canopy area in esca-symptomatic grapevine plants leads to lower canopy transpiration and mitigates water stress

Ninon Dell'Acqua,[1] Gregory A. Gambetta,[2] Megan K. Bartlett,[3] Régis Burlett,[4] Marie Chambard,[1] Sylvain Delzon,[4] Nathalie Ferrer,[1] Mathéo Pinol Daubisse,[1] Gabriela Sinclair,[3] Chloé E.L. Delmas[1,*]

[1]INRAE, Bordeaux Sciences Agro, ISVV, SAVE, Villenave d'Ornon F-33140, France
[2]EGFV, Bordeaux-Sciences Agro, INRAE, Université de Bordeaux, ISVV, Villenave d'Ornon 33882, France
[3]Department of Viticulture & Enology, University of California, Davis, CA 95616, USA
[4]INRAE, BIOGECO, Université de Bordeaux, Pessac 33615, France
*Author for correspondence: chloe.delmas@inrae.fr
The author responsible for distribution of materials integral to the findings presented in this article in accordance with the policy described in the Instructions for Authors (https://academic.oup.com/plphys/pages/General-Instructions) is: Chloé E.L. Delmas.

Abstract
In perennial plants, abiotic and biotic stresses may occur in combination and/or in sequence over many years, making understanding and predicting the combined effects of drought and pathogens on plant health and productivity a considerable challenge. In this study, we investigated the susceptibility of esca-symptomatic grapevines (*Vitis vinifera* L.) to drought. Esca is a grapevine vascular disease leading to decreased vineyard longevity worldwide. Using transplanted, naturally infected 20-yr-old "Sauvignon blanc" vines with known esca histories, we subjected esca-symptomatic and asymptomatic control vines to different drought periods. Whole-plant and leaf physiology, radial growth, anatomical traits, and long-term recovery were compared among treatments. Esca leaf symptoms were associated with stem xylem vessel occlusion, leaf drop, and decreased symptomatic leaf gas exchange, resulting in reduced canopy area and thus, lower whole canopy transpiration. When esca-symptomatic plants were subjected to drought, declines in water potential, CO_2 assimilation and stomatal conductance measured on green leaves, as well as canopy maximum transpiration, were delayed. Water stress did not cause a significant increase in stem xylem occlusion. The esca-symptomatic stems showed greater radial stem diameter recovery that coincided with faster regrowth of healthy new shoots at the top of the plant associated with a recovery of whole plant gas exchange. Esca mitigates the effects of drought through reduced canopy area, confirming an antagonistic interaction between these stresses. These results demonstrate the importance of combining abiotic and biotic stresses and understanding their interactions when studying dieback in the climate change context.

Introduction

Pathogen infection and drought are two major stresses affecting both natural and agricultural ecosystems (Wilcox et al. 2015) and are expected to increase under climate change (Trumbore et al. 2015; Chaloner et al. 2021; Singh et al. 2023). In this context, it has become increasingly important to evaluate the susceptibility of plants, especially perennials, to multiple environmental stresses in which the interaction between host, pathogens, and abiotic environment plays a crucial role over many years (Niinemets 2010; Ramegowda and Senthil-Kumar 2015).

Perennial fruit crops have been domesticated since the fourth millennium BC. Their cultivation is complicated since growers seek to simultaneously maximize yields, obtain high fruit quality, and maintain plant health and survival across many decades (Spiegel-Roy 1986). Grapevine (*Vitis vinifera* L.) was one of the first perennial fruit crops to be domesticated thanks to its ease of vegetative propagation (Spiegel-Roy 1986). Today it is one of the world's most valuable fruit crops and this value relies heavily on fruit quality especially with regard to the production of wine. Grape fruit quality is greatly impacted by the environment, including both abiotic and biotic stresses.

Drought is a peculiar abiotic stress in the context of wine production because it is both sought-after and feared. A moderate drought is often targeted because it encourages the production of quality red wine (Le Menn et al. 2019; Triolo et al. 2019). On the contrary, a severe drought can decrease growth and productivity (Gambetta et al. 2020). The physiological impact of intense drought is a phenomenon that has been studied extensively in plants (Brodribb and Cochard 2009; Gupta et al. 2020) and more specifically in grapevine (Gambetta et al. 2020; Hochberg et al. 2023).

Biotic stresses such as pathogens interact with abiotic stresses such as drought and modify the plant's physiological responses (Desprez-Loustau et al. 2006; Hossain et al. 2019). A specific example of these biotic–abiotic interactions is vascular disease and drought, as both stresses affect xylem water transport (McDowell et al. 2008; Torres-Ruiz et al. 2024). In grapevine, the vascular disease esca has been causing increasing concerns since the beginning of the XXI century, as one of the most damaging grapevine trunk diseases globally (Gramaje and Armengol 2011; Mondello et al. 2018). Esca is associated with symptoms including (i) different types of necrosis in the trunk (Mugnai et al. 1999), and (ii) a longitudinal brown band under the bark in the outer xylem

Received February 10, 2025. Accepted June 30, 2025.

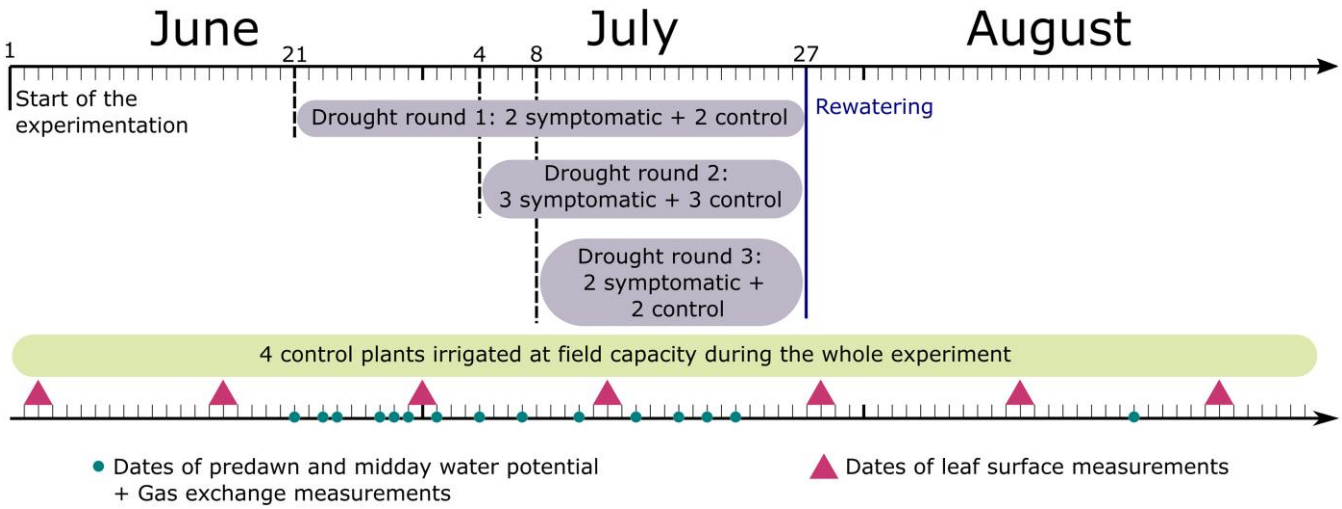

Figure 1. Schematic illustration of the experimental design. When at least two plants presented typical leaf scorch symptoms, irrigation was stopped for these plants and for at least two asymptomatic control plants. The same method was applied in three successive rounds for three groups of plants on three dates. The "Drought round 1" started on June 21 2022 and consisted of two symptomatic and two control plants. The "Drought round 2" started on July 4 2022 with three symptomatic and three control plants. The "Drought round 3" started on July 8 2022 with two symptomatic and two control plants. Four control plants were also well-watered (irrigated at field capacity) over the whole experiment. All plants were re-watered starting July 27 2022, corresponding to 35 d (round 1), 22 d (round 2), and 18 d (round 3) after the start of the dry-down. The points show the dates of the predawn and mid-day water potential and gas exchange measurements. The triangles show the dates of leaf area measurements.

tissue associated with (iii) typical leaf scorch symptoms, both appearing in the summer season (Lecomte et al. 2024).

Past attempts have been made to study the interaction between esca and drought using inoculations of pathogenic fungi causing trunk necroses. By inoculating with *Phaeomoniella chlamydospora*, it was observed that this pathogen induced distinct alterations in the physiological responses of grapevines to water stress across different cultivars. Specifically, "Cabernet Sauvignon" and "Zinfandel" exhibited lower leaf water potential (Edwards et al. 2007a, 2007b), whereas "Chardonnay" displayed higher leaf water potential (Edwards et al. 2007b), compared to noninoculated water-stressed vines. In order to study the interaction between water stress and esca leaf symptom formation in a more realistic system, a recent approach using naturally infected mature plants transplanted from the vineyard into pots has been developed. This experimental design enables the monitoring of leaf symptom development and whole-plant physiology under controlled conditions (Dell'Acqua et al. 2024, 2025) and has been used to compare drought and esca's underlying mechanisms (Bortolami et al. 2021b).

Drought and esca can have similar impacts on plant function through different mechanisms, and these effects can occur simultaneously or in succession within the same season. For example, both esca and drought reduce gas exchange and photosynthesis (Bortolami et al. 2021b), stem hydraulic conductivity (Choat et al. 2012; Bortolami et al. 2021a), alter stem radial growth rates (Zweifel et al. 2001; Dell'Acqua et al. 2024), and induce leaf shedding (Mugnai et al. 1999; Gambetta et al. 2020). However, stomatal conductance is reduced by declining water potentials during drought but not during the formation of esca leaf symptoms (Bortolami et al. 2021a; Dell'Acqua et al. 2024). Furthermore, hydraulic failure is caused by xylem embolism spread during drought (Dayer et al. 2020; Lamarque et al. 2023) and the formation of tyloses and gums in xylem in the case of esca (Bortolami et al. 2021a, 2023). The combined physiological effects of these stresses, whether positive, negative, or neutral, remain largely unknown.

Recent research has shown that grapevines experiencing long, intense drought do not express esca leaf symptoms, highlighting an antagonistic interaction (Bortolami et al. 2021b). However, in order to identify the importance of the sequence of these two stresses on this interaction, a question remains: Are grapevines already expressing esca leaf symptoms more susceptible to a drought event than asymptomatic vines? One of the hypotheses made in the literature is that vascular pathogens could accelerate drought-induced mortality by damaging the xylem vascular system, reducing water transport capacity, and causing phloem impairment and leaf shedding (Oliva et al. 2014). Vascular pathogenesis would increase the tension in the xylem during drought, increasing the likelihood of xylem embolism (Fischer and Peighami Ashnaei 2019). Another hypothesis postulates that the development of foliar symptoms, by leading to a physiological and molecular plant alteration (respectively through the reduction of whole-plant transpiration and the activation of secondary metabolism), mitigates the impact of drought.

The aim of this study was to test these two hypotheses and thus to determine the susceptibility of symptomatic plants showing typical esca leaf scorch symptoms to drought stress and recovery. To study esca pathogenesis under drought conditions, we used the experimental design introduced above of naturally infected 20-yr-old "Sauvignon blanc" vines transplanted into pots. Multiple traits were monitored during the whole experimentation: quantification of whole-plant and leaf gas exchange, predawn and midday water potentials, continuous stem radial growth, tylosis formation, and esca leaf symptom expression.

Results

Esca leaf symptom incidence

During the experiment (Fig. 1), eight plants out of 19 expressed esca leaf symptoms, with first symptoms expressed between June 8 and July 5 2022 (Fig. 2). One plant was of the apoplectic phenotype, with rapid and total defoliation, and was therefore not

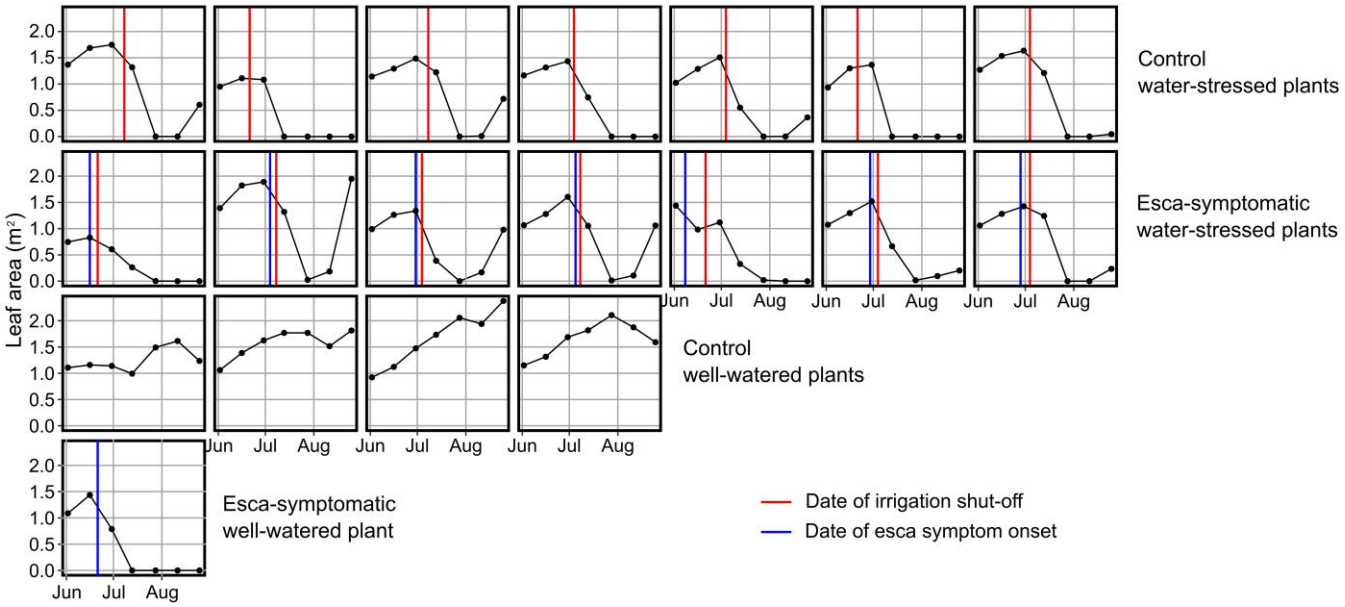

Figure 2. Evolution of whole plant leaf area (A_L) in control and esca symptomatic *V. vinifera* cv. "Sauvignon blanc" over time. The onset of esca leaf symptoms is indicated as a blue vertical line and the dry-downs begin at the red vertical line for water stressed plants. Each plant ($n = 19$) is represented by a single plot. Each horizontal grouping is a treatment: control water-stressed plants ("Control WS", $n = 7$), esca-symptomatic water-stressed plants ("Esca WS", $n = 7$), control well-watered plants ("Control WW", $n = 4$), and one esca-symptomatic well-watered plant ("Esca WW", $n = 1$).

subjected to water stress. None of the asymptomatic plants subjected to drought expressed symptoms later in the season. At the beginning of the drought experiment, symptomatic plants exhibited on average 56% of symptomatic leaves out of the total number of leaves remaining on the vine. Only 10% of the stems did not exhibit leaf symptoms.

Water status and gas exchange

Whole-plant transpiration

To assess whole-plant gas exchange, the 19 plants were placed on scales, and their mass was constantly monitored over the season. At the start of the experiment, the canopy area of future symptomatic and control plants were similar (i.e. 1.11 ± 0.08 (±se) m^2 ($n = 8$) and 1.10 ± 0.04 m^2 ($n = 11$), respectively; Fig. 2). The canopy area of symptomatic plants decreased at the onset of leaf symptoms, the canopy area of asymptomatic plants under drought decreased approximately at the onset of the dry-down, while the canopy area of control well-watered plants remained stable (Fig. 2).

Before esca symptom expression, whole plant (canopy) maximum transpiration (*Emax*) did not significantly differ between control and future symptomatic plants ($P > 0.05$, Wilcoxon test, Fig. 3). Between the onset of esca leaf symptoms and beginning of drought stress, *Emax* of symptomatic plants decreased while that of control plants remained constant (Fig. 3). At the start of the dry-down week, *Emax* of control plants was more than 1.5 times higher than *Emax* of symptomatic plants (Supplementary Table S1). During the dry-down, the transpiration of control plants decreased drastically and more rapidly than symptomatic plants with *Emax* being significantly lower during the first and second week after the dry-down started ($P < 0.05$, Wilcoxon test). Pictures of the plants and examples of weight differences 2 wk after irrigation was stopped are provided in Supplementary Fig. S1. We observed the same pattern for maximum canopy stomatal conductance (Supplementary Fig. S2).

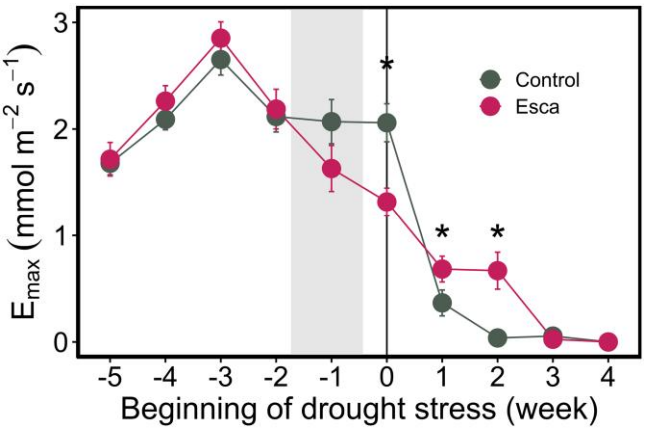

Figure 3. Whole-plant maximum transpiration in control and esca symptomatic *V. vinifera* cv. "Sauvignon blanc" during dry-downs. Evolution of the mean (±SE) whole-plant (canopy) maximum transpiration (E_{max}, mmol m^{-2} s^{-1}) relative to the beginning of the drought stress period in weeks (where 0 corresponds to the week when irrigation was stopped). Colors represent the different plant symptoms: dark gray for control water-stressed plants ($n = 7$) and dark pink for esca-symptomatic water-stressed plants ($n = 7$). The vertical gray band represents the period of esca symptom onset. The black vertical line indicates the beginning of the dry-down. The stars represent significant differences between control and symptomatic plants ($P < 0.05$, Wilcoxon test, see Supplementary Table S1 for detailed statistics).

Water potential and gas exchange

The water potential (ψ) was measured only on green leaves in control and symptomatic plants. Before the beginning of drought stress, predawn water potential (ψ_{PD}) ranged from 0 and −0.3 MPa and did not significantly differ between control and esca-symptomatic plants (Fig. 4A, Supplementary Table S2). After irrigation was stopped, ψ_{PD} decreased for both treatments, but much more rapidly for control plants than for symptomatic plants (Fig. 4A). One week after the beginning of the dry-down, ψ_{PD} was

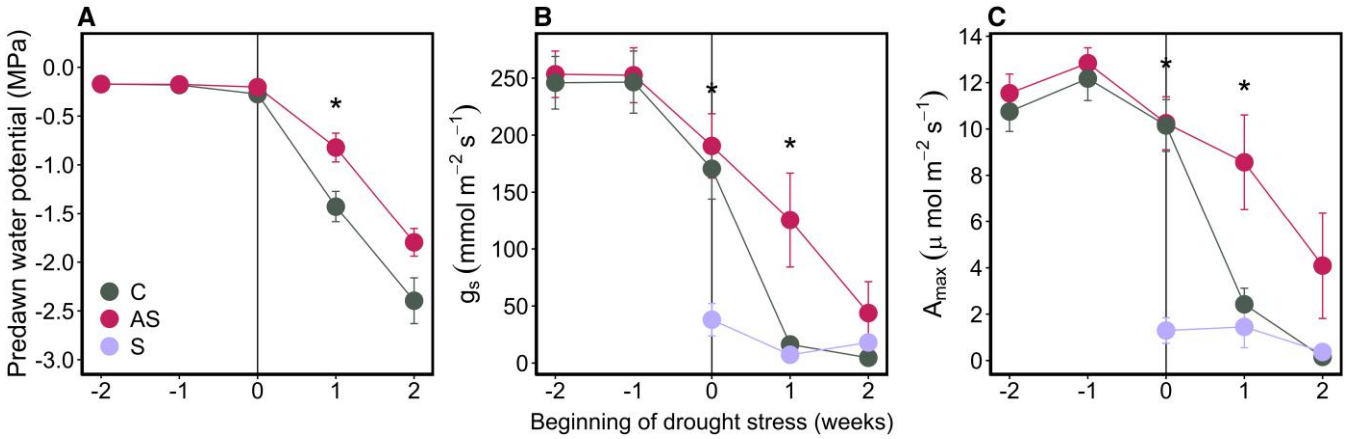

Figure 4. Water relations and leaf gas exchange before and after drought in *V. vinifera* cv. "Sauvignon blanc". **A)** Evolution of the mean (±SE) predawn water potential (ψ_{PD}) relative to the beginning of drought stress in weeks (where 0 corresponds to the week when irrigation was stopped). **B)** Evolution of the mean (±SE) leaf stomatal conductance (g_s, in mmol m^{-2} s^{-1}) measured with a porometer relative to the beginning of drought stress in weeks. **C)** Evolution of the mean (±SE) maximum net CO_2 leaf assimilation (A_{max}, in μmol m^{-2} s^{-1}) measured with a gas analyzer relative to the beginning of drought stress in weeks. ψ_{PD}, g_s and A_{max} were measured on green leaves ("AS") and symptomatic ("S") leaves on esca-symptomatic plants and control ("C") ones. Colors represent the different plant symptoms: dark gray for control water-stressed plants and dark pink for esca-symptomatic water-stressed plants. The black vertical line indicates the beginning of the dry-down. The stars represent significant differences between control and symptomatic plants ($P < 0.05$, Wilcoxon test). Sample sizes and statistics are detailed in Supplementary Tables S2 and S3.

significantly higher (less stressed) in esca-symptomatic plants than controls (Fig. 4A, Supplementary Table S2).

Prior to measuring minimum water potential at midday (ψ_L), we measured the stomatal conductance (g_s) and maximum leaf assimilation (A_{max}) on the same leaves. g_s and A_{max} were not significantly different between green leaves from symptomatic and asymptomatic plants before the dry-down (Fig. 4B and C, Supplementary Table S3). During the dry-down g_s and A_{max} dropped in green leaves from both symptomatic and control plants, but much more rapidly for control plants than for symptomatic plants (Fig. 4B and C). Symptomatic leaves demonstrated a significantly lower stomatal conductance compared to green leaves from symptomatic and control plants before drought (Fig. 4B, Supplementary Table S3) and remain low and stable during dry-down.

Regulation of water potential and stomatal conductance

The hydroscape delimits different periods during the dry-down (Fig. 5). During well-watered periods, the ψ_{PD} was always above −0.3 MPa and the ψ_L was above −1.5 MPa (Fig. 5). First, the reduction of the ψ_L was associated with a slight reduction of ψ_{PD}. Second, the ψ_L stabilized while the ψ_{PD} dropped until the ψ_{PD} and ψ_L reached the same values. Third, ψ_L and ψ_{PD} continued to decrease linearly. We observed this same pattern between control and esca-symptomatic plants (Fig. 5).

Furthermore, the g_s measured on green leaves between 10 and 12 h decreased with ψ_{PD} in the same way regardless of esca symptom expression (Fig. 6). In both control and symptomatic plants, we observed a decrease of stomatal conductance until the ψ_{PD} reached −1 MPa, after which stomatal conductance stabilized close to 0 mmol m^{-2} s^{-1}.

Using detached leaves installed in a drought box device, esca-symptomatic leaves presented a significantly lower leaf minimum conductance (g_{min}) than controls ($P < 0.05$, ANOVA, Supplementary Fig. S3).

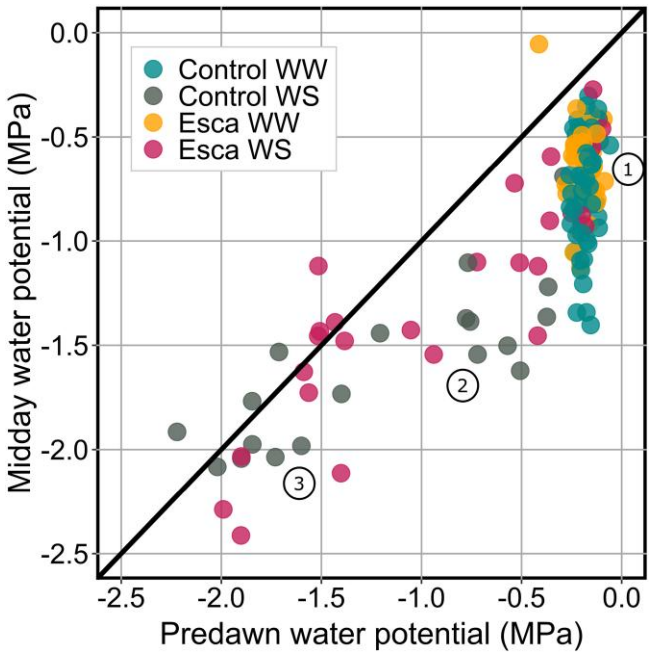

Figure 5. Hydroscape relationships between predawn water potential (ψ_{PD}) and mid-day water potential (ψ_l) during the drought experimentation. The hydroscape only includes ψ_{PD} and ψ_L that were measured on the same date. Colors represent the different plant symptoms: blue for control well-watered plants ("Control WW", $n = 60$ measurements of each ψ), gray for control water-stressed plants ("Control WS", $n = 22$), yellow for asymptomatic leaves from esca-symptomatic well-watered plants ("Esca WW", $n = 34$), and pink for asymptomatic leaves from esca-symptomatic water-stressed plants ("Esca WS", $n = 28$). All measurements were made on green healthy leaves. The hydroscape delimits different periods during the dry-down. The 1:1 relationship is indicated by a black line. First the reduction of the ψ_L was associated with a slight reduction of ψ_{PD} (1). Second, the ψ_L stabilized while the ψ_{PD} dropped (2) until the ψ_{PD} and ψ_L reached the same values and continued to decrease linearly (3).

Xylem occlusion by tyloses

We counted empty and occluded xylem vessels in entire stem cross-sections. The percentage of vessels occluded by tyloses in stems was significantly different between the four treatments combining water stress and esca leaf symptoms ($P < 0.01$, ANOVA; Fig. 7). We did not observe a significant difference

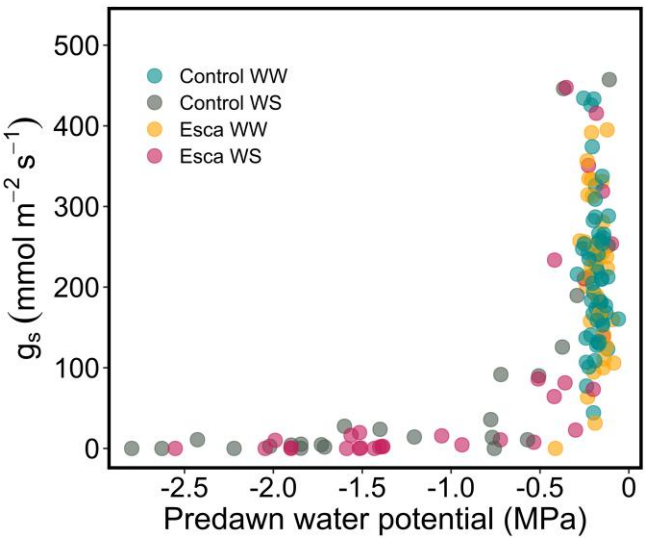

Figure 6. Relationship between predawn leaf water potential and stomatal conductance in *V. vinifera* cv. "Sauvignon blanc". The plot only includes ψ_{PD} and *gs* measurements that were measured on the same date. All measurements were made on green healthy leaves. Colors represent the different plant symptoms: blue for control well-watered plants ("Control WW", $n = 59$ measurements), gray for control water-stressed plants ("Control WS", $n = 24$), yellow for esca-symptomatic well-watered plants ("Esca WW", $n = 37$), and pink for esca-symptomatic water-stressed plants ("Esca WS", $n = 31$).

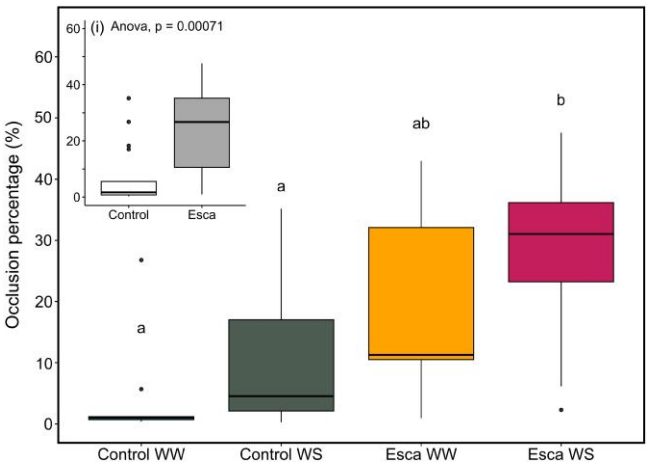

Figure 7. Percentage of occluded vessels in stem cross sections from plants under different treatment in *V. vinifera* cv. "Sauvignon blanc". Boxplots display the median and interquartile range, with whiskers extending to the minimum and maximum values, excluding outliers, which are shown as individual black points. Colors represent the different plant symptoms: blue for control well-watered plants ("Control WW", $n = 9$ stem cross-sections), gray for control water-stressed plants ("Control WS", $n = 9$ stem cross-sections), yellow for esca-symptomatic well-watered plants ("Esca WW" $n = 9$ stem cross-sections), and pink for esca-symptomatic water-stressed plants ("Esca WS", $n = 9$ stem cross-sections). Letters indicate statistical significance ($P < 0.05$) using Tukey's post-hoc comparisons. The inset graph (i) shows boxplots representing the percentage of occluded vessels in stem cross-sections from all control plants ($n = 18$ stems) and all esca symptomatic plants ($n = 18$ stems).

between well-watered (WW) and water-stressed (WS) ($P > 0.05$, ANOVA). However, control stems presented a significantly lower percentage of occluded vessels than stems with esca leaf symptoms (Fig. 7I, $P < 0.05$, ANOVA). Interestingly, we observed a gradation in the percentage of occlusion between treatments (i.e. 4 ± 3% in "Control WW", 9 ± 4% in "Control WS", 19 ± 5% in "Esca WW", and 27 ± 5% in "Esca WS").

Change in radial growth and water potentials recovery

Using continuous stem radial growth measurements, we found that the percentage loss in diameter (PLD, Supplementary Fig. S4) during the dry-down experiment was 2-fold higher in symptomatic plants but did not significantly differ between the two treatments ($P > 0.05$, ANOVA, Fig. 8). The recovery capacity in diameter 1 d after re-watering (R_{1dpr}) was significantly 4-fold higher in esca-symptomatic plants than controls ($P < 0.05$, ANOVA, Fig. 8). Water potentials measured at the trunk level using microtensiometers installed on one esca-symptomatic, one control vines subjected to the dry-down on July 4 2022 and one well-watered control vines demonstrated that trunk minimum water potential recovered above −0.3 MPa within 4 d in both esca-symptomatic and control plants (Supplementary Fig. S5).

Re-watering impacts on growth and pot water loss

Since irrigation resumed on the same date for all the drought rounds (Fig. 1), the different rounds did not have the same dry-down duration, and therefore were studied separately. After re-watering we observed growth for a higher number of buds in symptomatic plants than controls (Fig. 9A). This led to a larger leaf area in symptomatic plants than controls, associated with a higher mass loss (i.e. transpiration) during the day (Fig. 9B and C). The plants subjected to the shorter dry-down periods exhibited more and faster regrowth while none of the plants from the longest, 35-d dry-down, regrow (Fig. 9A and B).

Long-term impacts on esca leaf symptom development, stomatal conductance, and osmotic potential

The plants were also monitored in 2023 to assess their ability to recover. All the plants that were well watered and had no esca leaf symptoms during the 2022 season remained asymptomatic in 2023. The vine that had apoplectic esca symptoms in 2022 did not regrow and was scored as dead in 2023. Zero per cent, 67%, and 100% of control and esca plants survived from 2022 experimentation in the 35, 25, and 18 d dry-downs, respectively. In 2023, all esca-symptomatic plants from the 25 and 18 d dry-down remained symptomatic, and respectively 100% and 50% of the control plants remained asymptomatic.

The stomatal conductance (g_s) and osmotic potential at full hydration (π_0) were measured in 2023 in green leaves of grapevines that remained asymptomatic in 2023. We compared asymptomatic vines that were well-watered ("2022 Control WW") or water-stressed ("2022 Control WS") in 2022 and symptomatic vines that were water-stressed in 2022 ("2022 Esca WS"). "2022 Esca WS" vines demonstrated a g_s significantly higher in 2023 compared to "2022 Control WW" and "2022 Control WS" ($P < 0.05$, Tukey test, Fig. 10). g_s in two dates out of four was significantly higher in the "2022 Esca WS" than in "2022 Control WW" ($P < 0.05$, Tukey test, Supplementary Fig. S6). No difference in π_0 was found between treatments for any of the two measurement dates ($P > 0.05$, Tukey test, Supplementary Fig. S7).

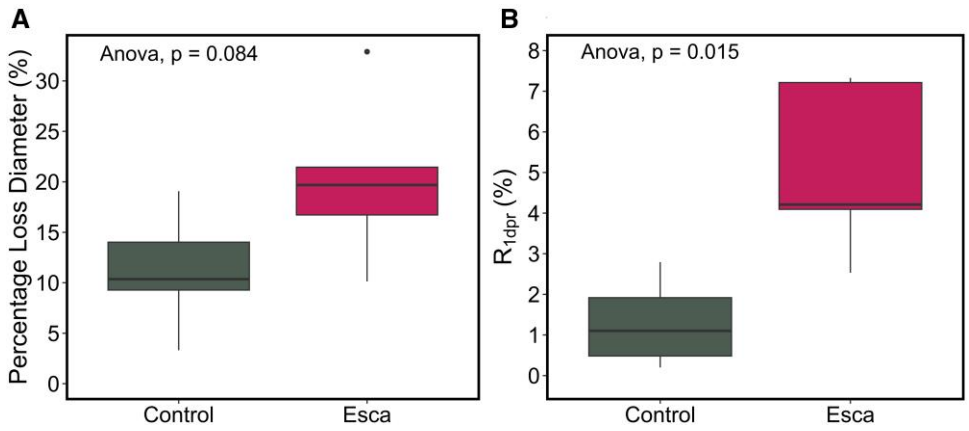

Figure 8. Radial growth differences between control and esca-symptomatic stems in *V.vinifera* cv. "Sauvignon blanc". **A)** Percentage loss in diameter (PLD, %) of control ($n = 5$) and symptomatic plants ($n = 5$) during the dry-down. The plants are those from the second and third rounds of drought (see Fig. 1). **B)** Recovery capacity 1 d post-re-watering (R_{1dpr}, %) of control ($n = 5$) and symptomatic plants ($n = 5$). Boxplots display the median and interquartile range, with whiskers extending to the minimum and maximum values, excluding outliers, which are shown as individual black points. *P* values are derived from an ANOVA test.

Discussion

In this study we investigated the impact of a vascular disease on the susceptibility of *V. vinifera* cv. "Sauvignon blanc" to drought and on its capacity to recover. We demonstrated that prior to the dry-down, esca pathogenesis resulted in reduced gas exchange at both symptomatic leaf and whole-plant scales. Symptomatic plants experienced a delayed and less intense water deficit due to the reduction in transpiring leaf area (reduced transpiration of symptomatic leaves and leaf shedding). Although esca causes stem xylem occlusions, this was not exacerbated by water deficit. After re-watering the esca-symptomatic stems demonstrated a higher recovery capacity that coincided with a faster production of healthy new shoots at the top of the plant, associated with a resumption of gas exchange at the whole plant scale. These results highlight that esca leaf symptoms delay and mitigate drought impacts in "Sauvignon blanc" through reduced canopy area. In the long term, the survival rate of plants was altered by the drought duration rather than the vine's health condition.

Symptom expression and drought impact

Impact of esca on leaf and whole-plant gas exchange and water status

The development of esca is characterized by the formation of leaf scorch symptoms and leaf abscission (Lecomte et al. 2012). In symptomatic vines, over 50% of the remaining leaves on symptomatic vines exhibited esca symptoms when irrigation was stopped. These symptomatic leaves showed a drastic reduction in gas exchange compared with asymptomatic leaves from symptomatic plants and from well-watered control plants. Before irrigation was stopped, no change in gas exchange was measured in asymptomatic leaves compared with control ones. These results are confirmed by previous studies on "Sauvignon blanc" vines (Bortolami et al. 2021b; Dell'Acqua et al. 2024) and on other varieties (i.e. similar results in "Cabernet Sauvignon", "Sangiovese" and "Trebbiano" varieties; Petit et al. 2006; Andreini et al. 2009). In this study, all symptomatic plants were subjected to the dry-down treatment. However, based on previous research, we can hypothesize that the decrease in transpiration would have continued for about 2 wk as demonstrated by Bortolami et al. (2021b) and Dell'Acqua et al. (2024). This decrease would probably have stabilized at a higher level than that of water stressed plants (Bortolami et al. 2021a, 2021b).

At the whole plant level, we demonstrated a reduction in transpiration with esca symptom expression without any change in water status. This reduction can be explained by reduced canopy area, a high percentage of symptomatic leaves with reduced gas exchange, and xylem occlusion, as previously demonstrated (Bortolami et al. 2021b; Dell'Acqua et al. 2024). These mechanisms could explain part or all of the differences in water stress response in our study. Additional hypotheses may include plant metabolism, regulatory, or signaling processes in responses to drought–disease interactions (Torres-Ruiz et al. 2024).

Comparison of drought response between control and symptomatic plants

During the dry-down, we demonstrated a delayed impact of drought in symptomatic vines compared to control vines defined by a delayed whole-plant transpiration reduction and a delayed decrease in green leaf gas exchange and water status. In symptomatic plants, the high ratio of symptomatic leaves with closed stomata (low and stable leaf gas exchange) has reduced the potential transpiration of symptomatic plants, likely resulting in the delayed impact of drought on symptomatic plants compared to controls. In addition, we found a lower g_{min} in symptomatic leaves suggesting that even when stomata are completely closed these leaves will lose water more slowly than control leaves (Supplementary Fig. S2). This could be due to an alteration in the structure of the cuticle or the guard cells of the stomata.

In numerous studies, emphasis is often placed on the possible synergistic effect between drought and disease (Desprez-Loustau et al. 2006; Oliva et al. 2014). However, other studies have highlighted the importance of stress severity, timing, and the type of causative agent (Ramegowda and Senthil-Kumar 2015). We applied a range of stress levels, from those experienced regularly in the field to those that would be considered extremely severe, although not unseen in viticultural situations. This level of water stress (characterized by intensive water potential measurements) was very similar to that monitored in the field during recent periods of summer droughts (Charrier et al. 2018). Some evidence for pathogen-induced mitigation of drought has been demonstrated. For example, *Nicotiana benthamiana* plants infected with three

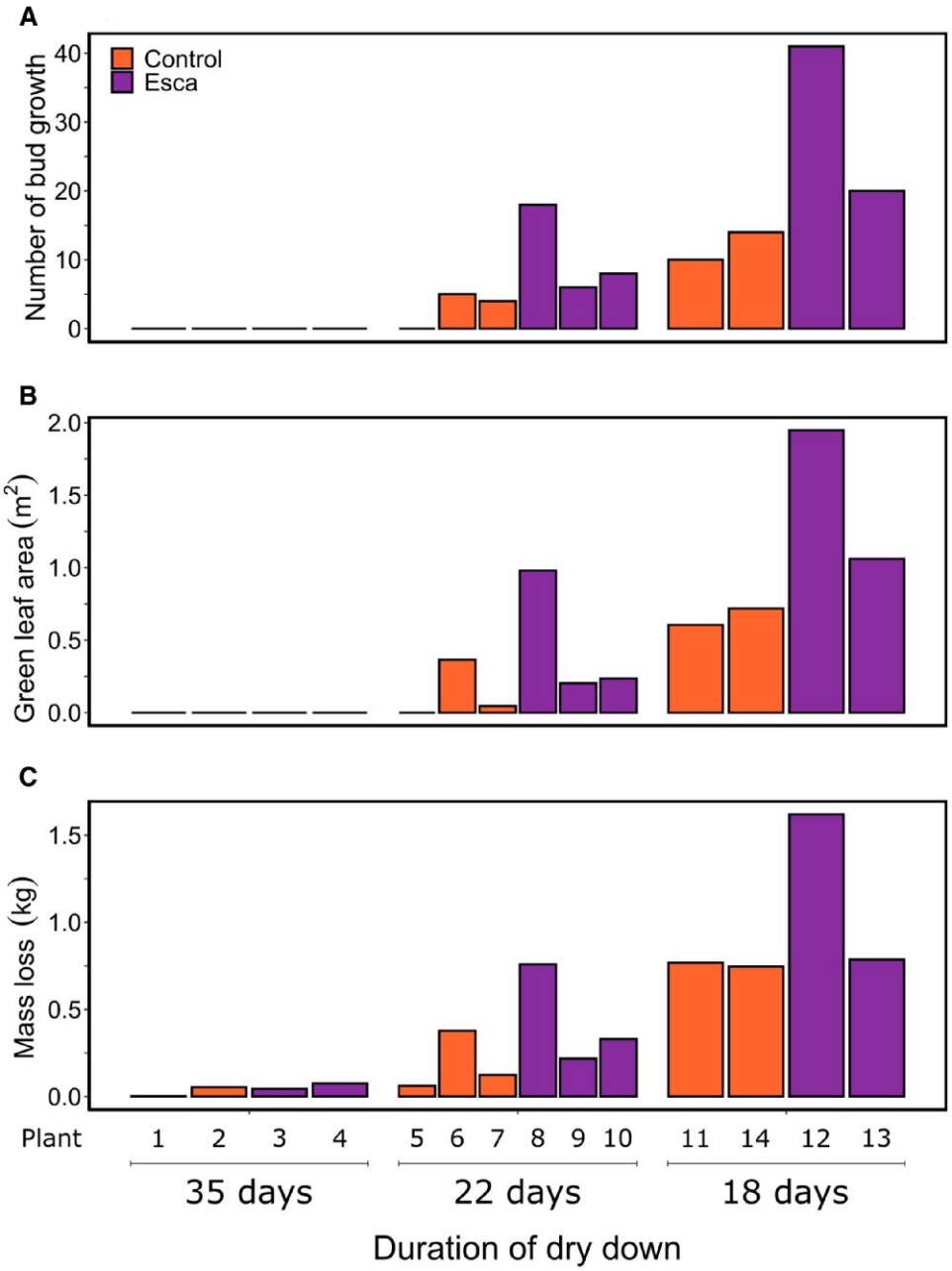

Figure 9. Mass loss and the green leaf area after 1 mo of re-watering in *V. vinifera* cv. "Sauvignon blanc". **A)** Number of bud growth August 22 2022. **B)** Total green leaf area (in m^2) during August 25 2022. **C)** Total water loss (in kg) during August 26 2022. Each bar represents one plant numbered from 1 to 13 on the x-axis and grouped according to dry-down duration (35, 22 or 18 d as detailed in Fig. 1).

different viruses showed delayed appearance of leaf wilting and stem dehydration under combined virus and drought compared to drought alone (Xu et al. 2008). Similar to our research, infected plants exhibited lower transpiration rates due to partial stomatal closure, resulting in better water retention in leaf tissues. Moreover, infected plants showed increased accumulation of osmoprotectants such as glucose, fructose, and sucrose (Xu et al. 2008). A modification in leaf composition was also noted in the case of esca pathogenesis (Fontaine et al. 2016), with an increase in fructose and glucose in symptomatic leaves but accompanied by a loss of sucrose (Bortolami et al. 2021b). In addition, crosstalks between abiotic and biotic stress responses had been documented in the stress signaling networks (Fujita et al. 2006) and could be involved in drought response in esca symptomatic plants. We can hypothesize in particular that abscisic acid (ABA), which has a well-known role in plant response to drought (Fujita et al. 2006) and a putative role in plant–pathogen interactions (Cao et al. 2011), could play a key role in esca–drought interaction. Esca symptomatic plants and/or pathogenic fungi could produce ABA during pathogenesis (Chanclud and Morel 2016) contributing to the observed decline in vine transpiration after symptom onset and before we started the dry-down.

Interaction between physiological parameters

The hydroscape allows the study of plant responses to soil drying by comparing the relationship between ψ_{PD} and ψ_L (Martínez-Vilalta et al. 2014). The difference between the ψ_{PD} and ψ_L is linked to the

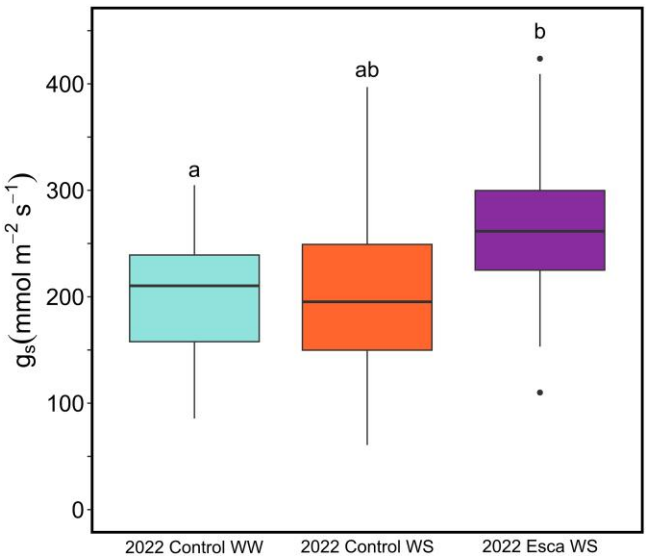

Figure 10. Mean stomatal conductance per plant (g_s) 1 yr post-recovery: comparison between *V. vinifera* cv. "Sauvignon blanc" plants undergoing different stresses during 2022. Colors represent the different plant symptoms from 2022: light blue for plants that were well-watered control in 2022 ("2022 Control WW", three plants, 48 measurements), light gray for plants that were water-stressed control in 2022 ("2022 Control WS", four plants, 63 measurements), and light pink for plants that were water-stressed esca-symptomatic in 2022 ("2022 Esca WS", three plants, 49 measurements). Letters indicate statistical significance ($P < 0.05$) using Tukey's post-hoc comparisons.

regulation of the plant's water status in response to soil moisture content (Charrier 2020). In our study, we did not identify any differences in the behavior of symptomatic and control plants during the dry-down. We observed the same three typical phases in the relationship between ψ_{PD} and ψ_L: first, ψ_L decreased much more rapidly than ψ_{PD} indicating a very loose regulation of ψ_L under well-watered conditions; then ψ_L plateaued corresponding to stomatal closure; finally, ψ_{PD} and ψ_L decreased and converged, indicating a loss of regulation (Charrier 2020; Knipfer et al. 2020) in symptomatic and control plants during dry-downs. Furthermore, the effect of water potential on stomatal conductance was the same in both control and symptomatic plants. Thus, the stomata of symptomatic plants (measured on green leaves) were not more or less sensitive than those of control plants in response to the water potential at which they operate. This suggests that the mitigation of drought in symptomatic plants is almost entirely due to reduced whole-plant transpiration.

Plant defense response to multiple stresses

The production of occlusion in the xylem vessels is a defense response of the plant. Vessel occlusion can be due to the formation of tyloses or gum deposition (De Micco et al. 2016) and occurs during xylem aging and in response to various abiotic stresses (frost, Cochard and Tyree 1990; flooding, Davison and Tay 1985) and biotic stresses (pathogen infection, Fanton androdersen 2021; Bortolami et al. 2021a). Recent research has shown that occlusions during esca result from tyloses, which are induced during other processes by ethylene (Sun et al. 2007, not yet established during esca), and not air embolism (Bortolami et al. 2021a). We confirmed here that symptomatic plants exhibited a significantly higher level of occlusions than controls confirming previous studies (Bortolami et al. 2021a; Dell'Acqua et al. 2024). However, drought does not exacerbate this phenomenon: no difference in percentage of occlusion between well-watered and water-stressed stems was found. Considering both stresses, we observed a gradient of vessel occlusion percentage with esca-symptomatic water stressed plants having the most occluded stems. This research studied this trait under multistress conditions in grapevines. Further research focusing on the role of ethylene during multistress tylose formation would open perspectives to understand the underlying mechanisms of tylose formation.

The recovery process

Short-term recovery

We re-watered (gradually until 90% of field capacity) all the plants on the same dates resulting in different dry-down durations of 35, 22, and 18 d finding significant differences between control and symptomatic plants in their short-term recovery capacity. Trunk minimum water potential returned to nonstress levels within 4 d for both control and symptomatic plants following re-watering. Interestingly, the trunk minimum water potential was twice lower (more negative) in the symptomatic plant than in the control plant before re-watering. Trunks of symptomatic plants are usually more necrotic than controls (Maher et al. 2012; Ouadi et al. 2019), likely leading to higher resistance to water transport and thus lower water potentials. However, this result is based on only one microtensiometer per treatment, hampering our ability to make firm conclusions.

Stem radial diameter of symptomatic plants was able to recover more quickly than control ones, despite not significantly different PLD during the dry-down periods. The ability of the stem to recover is not the only requirement for the stem to be able to produce new shoots. Taken together with the fact that the drop in leaf water potential was delayed in esca-symptomatic plants (i.e. were less stressed than control plants for a given dry down duration, in contrast to trunk water potentials) it explains the faster recovery and regrowth of the esca-symptomatic vines. Grapevine is characterized by its hydraulic vulnerability segmentation between stems and leaves which protects the perennial tissues from drought-induced embolism (Tyree and Ewers 1991; Choat et al. 2005; Charrier et al. 2018; Lamarque et al. 2023). Buds are strongly connected to the cambium, and it is thought that maintenance of these tissues ensures the ability of a plant to regrow, and thus survive (Barigah et al. 2013). We can therefore assume that the cambium and buds will be equally protected by the vine's segmentation capacity. Moreover, recently it has been shown that despite the significant production of occlusion in symptomatic stems, the cambium remained functional and symptomatic plants are able to produce new green shoots after esca pathogenesis through the production of new vessels (Dell'Acqua et al. 2024). Such resilience mechanisms were associated with an altered timing and sequence of stem growth periods (Dell'Acqua et al. 2024). We can hypothesize that the alteration of growth dynamics in esca-symptomatic stems, which is often associated with a delayed lignification, would be involved in the higher recovery of the symptomatic stems to drought through a prolonged cambial activity in esca symptomatic plants in comparison to controls.

Recent research showed the same ability of the plant to produce new xylem vessels after drought (*Eucalyptus saligna*, Gauthey et al. 2022). Therefore, it appears that vines maintain a strong regrowth capacity even if vines experiencing the multiple stresses exhibited a higher level of tylose occluded vessels in stems. This suggests that it is the intensity (i.e. minimum water

potential) and duration of the drought stress that plays the critical role in recovery and not necessarily hydraulic capacity per se.

We demonstrated that the longer the irrigation was stopped, the less the vines were able to initiate growth from buds. Moreover, the symptomatic plants presented a greater number of bud regrowth than controls. The healthy green leaf area was largely associated with these new shoots and therefore induced higher healthy leaf area in symptomatic vines. This difference in post-recovery vigor led to greater transpiration and photosynthesis as evidenced by continuous weighing on the mini-lysimeter platform. Moreover, the shorter the dry-down period, the faster and greater the resumption of transpiration (Fig. 8). We conclude that in the short-term esca symptomatic plants recovered faster because they were subjected to lower levels of stress or because esca is affecting the hormonal regulation of growth.

Long-term recovery

Numerous articles evaluated the drought's long-term impact by assessing the plant's response to a new drought and evaluating the susceptibility of the plant to sequential droughts (Hochberg et al. 2017; and Tombesi et al. 2018 in *V. vinifera*), but to our knowledge there was no research performed to evaluate the impact of coupled stresses on plant physiology during the following non-stressed season.

In the long term, the rate of plant survival depended more on the duration of the drought period than on the health condition of the vine. Esca did not impair the grapevine's ability to survive 1 yr after the experiment. This result could be explained by the less negative water potential observed in esca symptomatic plants compared to control water-stressed plants or by the less detrimental metabolic consequences of stress under esca than under drought. Furthermore, the drought did not inhibit the appearance of symptoms the following well-watered year. We also found that plants that had experienced drought stress only presented similar stomatal conductance 1 yr later than controls. This result is consistent with the findings of Herrera et al. (2024) who showed that 2 yr of short drought (i.e. 25 d at −1.5 MPa) did not cause any changes in anatomy and gas exchange in the following well-watered year. However, plants subjected to combined drought and esca stresses presented higher stomatal conductance the year after but similar leaf drought tolerance (estimated from the leaf osmotic potential at full hydration; Bartlett et al. 2012). We can hypothesize that plants subjected to the two stresses compensated for resource depletion the year after through enhanced gas exchanges. To test this hypothesis, further research should be realized focusing, for example, on carbon storage, photosynthesis, and anatomical measurements.

Conclusion

To conclude, we demonstrated that esca leaf symptom expression mitigated the response to drought. This antagonistic interaction between the two stresses was mainly due to the loss of the transpired leaf area associated with esca development. Esca-symptomatic vines suffered lower levels of stress compared to controls, resulting in a faster physiological recovery. Future studies should investigate the importance of the timing between esca symptoms expression and drought, and thus for different varieties. These results demonstrate the importance of studying the interaction between abiotic and biotic stresses in the context of perennial plant dieback and climate change.

Materials and methods

Plant material

We used 19 vines of *V. vinifera* L. cv. "Sauvignon blanc" (316 clone) grafted on the Fercal rootstock from a Pessac Leognan vineyard planted in 2000. The plants were uprooted in 2022 ($n = 12$) and 2021 ($n = 7$). The presence of esca leaf symptoms have been monitored in this vineyard at the plant level since 2012 following Lecomte et al. (2012). Plants were uprooted during late winter and transferred into 20 l pots as described in Bortolami et al. (2019). Transplantation is the only method allowing the study of natural esca symptom development on mature plants outside the field. Plants were pruned to retain six one-bud spurs. Before the beginning of the experimentation, clusters were removed and during the experimentation secondary shoots were removed (except after re-watering). In the greenhouse, plants were irrigated with nutritive solution (0.1 mM $NH_4H_2PO_4$, 0.187 mM NH_4NO_3, 0.255 mM KNO_3, 0.025 mM $MgSO_4$, 0.002 mM Fe, and oligo-elements [B, Zn, Mn, Cu, and Mo]). Environmental conditions were monitored every 15 min using temperature and humidity probes (S-THB-M002, Onset) and global radiation sensors (S-LIx-M003, Onset) connected to a data logger (U300-NRC, Onset). During the experiment period the vapor pressure deficit (VPD) was on average 0.906 ± 0.003 kPa.

Lysimeter phenotyping platform experiment

The 19 plants were randomly installed in four rows in a mini-lysimeter greenhouse phenotyping platform (Bord'O platform, INRAE Bordeaux), on individual scales (CH15R11, OHAUS type CHAMP) measuring their weight continuously over the 3 mo experiment. Well-watered (control) plants were automatically watered to field capacity twice a day. To determine field capacity, we immersed the plants into water for 15 min, let them drain, and weighed the plants the day before beginning the experiment. Pots were sealed into bags over the entire experiment to measure evapotranspiration from only the plants. The dry-down treatments are described below ("water deficit management").

Symptom notation, plant phenology, and leaf area

Leaf symptom expression was monitored weekly over a 2 mo period at the leaf, stem, and whole plant levels to start the dry-down treatments just after symptom onset. The phenotypes scored at the leaf or stem level were separated into three classes: "C", leaf or stem from control plants (asymptomatic during the whole season); "AS", asymptomatic leaf or stem from symptomatic plants (both before and after symptom appearance), and "S", symptomatic leaf or stem (presenting leaf scorch symptoms) samples. The percentage of symptomatic leaves per plant was assessed within the first week of the start of the dry-down by counting the number of healthy and symptomatic leaves per stem. Note that esca already led to leaf abscission at that stage for some of the plants. The development and phenology of new buds was also monitored, by counting the number of new shoots produced over time after re-watering.

To estimate total leaf area per plant (A_L, m^2), we measured the leaf midrib length every 2 wk for all the leaves of each plant. A_L was estimated from the relationship obtained between leaf midrib length and leaf area of ~150 leaves (measured with a leaf area meter Model LI-3000, LI-COR, Lincoln, Nebraska, USA). After drought stress, the presence of green regrowth was determined.

Water deficit management

When at least two plants presented typical leaf scorch symptoms, irrigation was stopped for these plants and two asymptomatic (control) plants. This method was applied in three successive rounds to three groups of plants on three dates (Fig. 1).

The first round of drought started on June 21 2022 and consisted of two symptomatic and two control plants. The second round started on July 4 2022 with three symptomatic and three control plants (Fig. 1). The third round of drought started on July 8 2022 with two symptomatic and two control plants. In addition, four control plants were irrigated at field capacity over the entire experiment. A recovery period was started 35 d (round 1), 22 d (round 2), and 18 d (round 3) after the start of the dry-down by gradually reinstating the water supply with daily irrigation at 75% of field capacity for 5 d, 80% for 9 d, and finally at 90% until the end of the experimentation.

Whole-plant gas exchange

Vine transpiration per leaf area (E in mmol m^{-2} s^{-1}) was calculated as:

$$E = \frac{\Delta_w}{A_L} \times \frac{1}{MW},$$

where Δ_w is the change in weight within a 3-d focal period (g s^{-1}), A_L is the leaf area (m^2) described above, and MW the molecular weight of water (18 g mol^{-1}). To avoid aberrant values, Δ_w measurements were filtered to range from 0 to −0.5 g s^{-1}, and during drought Δ_w values > −0.02 were set to 0. When $A_L = 0$, the value of 0.0001 was assigned to allow calculations.

The whole plant (canopy) conductance (G_c in mmol m^{-2} s^{-1}) was then calculated as:

$$G_c = K_G(T) \times \frac{E}{D},$$

where $K_G(T)$ is the conductance coefficient (115.8 + 0.4236T, kPa m^3 kg^{-1}), E is transpiration (E in mmol m^{-2} s^{-1}), and D is the VPD (kPa) calculated from recorded relative humidity (in %) and T (in °C). The G_c values were filtered to exclude values where mean daily G_c was <800 mmol m^{-2} s^{-1}, and values measured under less than saturating radiation (photosynthetic photon flux density (PPDF) < 500 μmol m^{-2} s^{-1}) and excessive D (≥0.6 kPa).

Leaf water potential

Mid-day (13 to 15 h) and predawn (before sunrise from 5 to 6 h) leaf water potentials (ψ_L and ψ_{PD}) were measured with a pressure chamber (Scholander). Mature, sun-exposed leaves from the middle of the stem were measured on 14 dates from June 21 2022 to July 22 2022. Leaf water potentials are not measurable in symptomatic leaves due to occlusions (tyloses), as discussed in Bortolami et al. (2019), thus all measurements were made on green leaves. We measured a total of 151 ψ_{PD} and 211 ψ_L. We used a hydroscape analysis to compare the relationship between ψ_{PD} and ψ_L in each treatment and study plant responses to soil drying.

Trunk water potential

To measure the plant water status after re-watering, microtensiometers (FloraPulse, Davis, California, USA) were embedded into the grapevine trunk of three potted grapevines, one control well-watered, one symptomatic dry-down plants, and one control water-stressed grapevines. The sensors were positioned on a non-necrotic part of the trunk and protected from the sunlight. Trunk measurements with microtensiometer were recorded every 5 min using Campbell 1000× data logger. The minimum and predawn water potential were recorded as the minimum and maximum water potential measurements of the day, respectively.

Osmotic potential

In 2023, we measured the leaf osmotic potential (π_0) for control plants that survived the 2022 drought experiment ($n = 10$) to test for carry-over effects on leaf drought tolerance via the water potential at the turgor loss point (Bartlett et al. 2012). Two leaves per plant were excised, re-cut under water, and rehydrated overnight by submerging the petiole of each leaf in Eppendorf tubes filled with DI water. Individual Whirl-Pak plastic bags were placed over each leaf to prevent transpiration. π_0 was measured using an osmometer (Vapro 5600—EliTechGroup) on leaf discs 0.5 cm in diameter that had been flash-frozen in liquid nitrogen. The osmometer was set to "auto-repeat" mode and measurements were recorded until the device stabilized and the difference between two measurements was less than or equal to 5 mmol kg^{-1}.

From fully hydrated leaves we calculated the TLP mean per plant and date from the osmotic potential following methods previously described by Bartlett et al. (2012). Two measurement campaigns were carried out at the beginning of the season at the end of leafing (May 22 2023) and a second 2 wk later (June 7 2023) to test for osmotic adjustment. We compared asymptomatic vines that were well-watered ("2022 Control WW", three plants, six samples) or water-stressed ("2022 Control WS", four plants, eight samples) in 2022 and symptomatic vines that were water-stressed in 2022 ("2022 Esca WS", three plants, six samples).

Leaf gas exchange

Photosynthesis was measured from 9 to 12 h on mature well-exposed leaves from the middle of the stem using the TARGAS-1 portable photosynthesis system (PP Systems). Cuvette Photosynthetic Active Radiation was set to optimize photosynthesis (1,500 μmol m^{-2} s^{-1}). The light-saturated photosynthetic rate, A_{max} (μmol m^{-2} s^{-1}) was recorded on one mature leaf (or two for symptomatic plant: "AS" and "S"). In total, we measured 227 leaves from 19 plants between June 7 and July 22, across 15 different dates.

Stomatal conductance (g_s, mol m^{-2} s^{-1}) was measured on the same green leaves and sampling dates as photosynthesis from 10 to 12 h with a Li-600 (Licor). In total, we measured 300 leaves from 19 plants between June 7 and July 22, across 15 different dates. When possible, these measurements were taken on the same leaves used for photosynthesis assessments. We also measured stomatal conductance in 2023, for the same leaves as osmotic potential. We measured the stomatal conductance on two leaves per plant ($n = 10$), including each leaf prior to being sampled for osmometry, on three dates between June 6 and July 18 2023.

Leaf minimum conductance

Water loss in 24 detached leaves was measured with a custom set-up adapted from the drought box device (Billon et al. 2020). Two types of leaves were sampled: "C", leaves from control plants (asymptomatic between June and October 2022, $n = 8$) and "S", esca symptomatic leaves (presenting scorch symptoms, $n = 16$). To monitor weight loss continuous logging of micro load cells by a Wheastone bridge board was performed (1046_OB, Phidgets Inc., Canada). Our setup consisted of 24 load cells, with a range of 0 to 100 g (3139_0, Phidgets Inc., Canada) enclosed in a 1,200 l growth chamber (Fitoclima 1200, Aralab, Portugal). Temperature and relative humidity (RH) in the chamber were set to 25 °C and

60% respectively, resulting in an air VPD of ca. 1.26 kPa. During measurement, samples were illuminated from the top and from the bottom with a Photon Flux Density at 400 μmol m^{-2} s^{-1}. In order to prevent direct desiccation from the petiole cut end they have been immersed in paraffin wax prior to the experiment. Samples were automatically weighed every 5 min. Data acquisition, calibration, and metadata management were conducted with a custom software from the University of Bordeaux (Cuticular v1, University of Bordeaux).

Turgid weight (TW) and area (A_{leaf}) of each individual leaf were measured before the water loss measurements in the climatic chamber. Weight measurements were performed with a four-digit balance (Pioneer, Ohaus, USA). Leaf area was obtained from images taken with a calibrated flatbed scanner (v850 pro, Epson, Japan) and analyzed with a dedicated software (Winfolia, Regent Inst., Canada). At the end of the measurement, leaves were put in an oven at 65 °C for 72 h and dry weight (DW) was measured. The relative water content (RWC) was then computed for each mass value (fresh mass; FW) during the dehydration process using the following equation:

$$RWC = \frac{FW - DW}{TW - DW.}$$

Leaf minimum conductance was computed for each leaf as:

$$g_{min} = \frac{dw}{dt} \times \frac{P_{atm}}{M_{H2O} \times A_{leaf} \times VPD,}$$

where dw/dt is the slope of the curve of the weight (in g) in function of time (in s), M_{H2O} is the molecular weight of water (18.01 g mol^{-1}), A_{leaf} is the projected leaf area of the sample, P_{atm} is the atmospheric pressure in the chamber (ca 101.9 kPa) and VPD is the measured water pressure deficit of the air in the chamber (in kPa).

A python program has been used to compute minimum conductance in a reproducible and efficient manner (gminComputation, University of Bordeaux). It enables computation within a set of given ranges of RWC.

Stem anatomy

On July 8 2022, we sampled a middle internode from 12 stems from three different plants per treatment and made three 40 μm cross sections at least 1 cm apart using a GSL-1 microtome (Gärtner et al. 2014). The sections were then placed in a 0.5% safranin/astrablue solution for about 2 min, rinsed twice with absolute ethanol, impregnated with xylene, and then mounted between slide and coverslip with Histolaque (Histolaque LMR) to obtain permanent slides. The section was then photographed using a binocular magnifier, Nikon SMZ1270 camera and NIS-ElementsD software. For each sample, we selected the clearest, best stained, and most complete cross-section for analysis, and calculated the percentage of occluded vessels by counting all occluded and non-occluded vessels in each of the 36 cross-sections.

Stem growth measurements

The stem diameter dynamics of the 19 grapevines was continuously monitored using stem dendrometers (DD-S2 Dendrometer, Ecomatik), as in (Dell'Acqua et al. 2024). One dendrometer was installed on one randomly selected shoot per vine among the eight stems, on the first basal internode that was long and strong enough to support it. All dendrometers were connected to dataloggers (DL-18, Dendrometer data logger, Ecomatik) and the data were recorded hourly and retrieved weekly from June to October 2022 with HOBOware software. The raw dendrometer data for each vine were checked and cleaned using the "treenetproc" package in R software. Since the dendrometers were placed at the beginning of the season, without knowing the future disease incidence, the analysis ultimately included four well-watered and seven water-stressed control stems, and one well-watered and eight water-stressed stems presenting leaf symptoms.

The stem diameter evolution was estimated using (i) the Percentage Loss in Diameter (PLD, in μm) during the dry-down experiment (Lamacque et al. 2020):

$$PLD = \frac{D_{max} - D_{min}}{D_{max}} \times 100;$$

and (ii) the diameter recovery the night after re-watering (R_{1dpr}, in μm) (Lamacque et al. 2020):

$$R_{1dpr} = \frac{Dr - D_{min}}{D_{max}} \times 100$$

where D_{max} and D_{min} are the maximum and minimum diameters (D) immediately before the dry-down treatment starts and at the peak of drought stress during the dry-down event and Dr is the diameter the day after re-watering (see Supplementary Fig. S4).

Statistical analysis

First, we compared E_{max}, G_{cmax}, g_s, A_{max}, and ψ between the control and esca vines for each week before and after the start of the dry-down with Wilcoxon tests (Supplementary Table S1). Second, we compared occlusion percentages between all four treatments ("Control WW", "Control WS", "Esca WW", "Esca WS") and the watering and disease treatments separately with ANOVAs and post-hoc Tukey HSD tests, adjusted for multiple comparisons (Fig. 6). We also used ANOVAs to compare R_{1dpr}, PLD, and g_{min} measurements between control and symptomatic plants (Fig. 8, Supplementary Fig. S3). We used a linear mixed-effect model to compare mean g_s per plant, measured in 2023, between watering treatments for control leaves and between disease categories for water-stressed leaves. The models included the date variable set as a random effect and the treatment as fixed effect, and was followed by a Tukey HSD test adjusted for multiple comparisons. Finally, for each date of g_s and π_0 measurements in 2023, we used a ANOVAs and post-hoc Tukey HSD tests, adjusted to compare between treatments. Before each ANOVA analysis, normality was verified through the Levene test. All statistical analyses were performed using R (version 4.2.2).

Acknowledgments

We thank the experimental teams of UMR SAVE and UMR EGFV (INRAE, Bordeaux, France) for providing the materials, logistics, and assistance during the experimentation. We thank Jérôme Jolivet and Sebastien Gambier (UMR SAVE) for providing technical knowledge and support for plant transplantation and maintenance; Marie-Christine Médalin, Nadège Cialti and Valérie Villars (UMR SAVE) for their support in the administrative management of the projects. We thank Nabil Girollet, Guillaume Pacreau, and Nabil Zirari for the maintenance of the mini-lysimeter greenhouse phenotyping platform (Bord'O platform, INRAE Bordeaux). We thank Uri Hochberg (Volcani Center) for insightful discussions on the analysis of microtensiometer data. We thank Patrick Leger (UMR BIOGECO) for the dendrometer's expertise, support, and materials. Minimum leaf conductance measurements were performed at PHENOBOIS platform (Université de Bordeaux/INRAE, Pessac, France).

Author contributions

N.D.A., C.E.L.D., and G.A.G. designed the experiments; N.D.A., C.E.L.D., and N.F. conducted the esca symptom notations and conducted the setting-up of the dry-down; N.D.A., M.P.D., M.C., and N.F. carried out the samplings, manage the dendrometers over the season; measured leaf gas exchange and leaf area; N.D.A., N.F. measured midday water potentials and conducted the histological preparation; M.P.D., G.S. measured osmotic water potentials; R.B. measured the leaf minimum conductance and supervised the installation of microtensiometers; N.D.A. measured predawn water potentials; processed the optical images on ImageJ; analyzed optical images, and analyzed all data sets from scales, leaf areas, dendrometers, weather stations, leaf gas exchange, and water potentials; N.D.A. wrote the first draft of the article under the supervision of C.E.L.D. and G.A.G. All authors participated in scientific discussion regarding the experimentations and methodologies used, edited, and agreed on the last version of the article.

Supplementary data

The following materials are available in the online version of this article.

Supplementary Figure S1. Images of one control plant and one esca-symptomatic plant taken 2 wk after irrigation was stopped.

Supplementary Figure S2. Whole-plant maximum conductance (G_{cmax}) in control and esca-symptomatic *V. vinifera* cv. "Sauvignon blanc" during a dry-down.

Supplementary Figure S3. Comparison of minimum stomatal conductance (g_{min}) between control and esca-symptomatic leaves in *V. vinifera* cv. "Sauvignon blanc".

Supplementary Figure S4. Schematic representation of the stem diameter evolution during a dry-down and a re-watering.

Supplementary Figure S5. Trunk minimum water potential in control well-watered and water-stressed vines and esca-symptomatic *V. vinifera* cv. "Sauvignon blanc" water-stressed vines during recovery.

Supplementary Figure S6. Stomatal conductance (g_s) measured in 2023 of *V. vinifera* cv. "Sauvignon blanc" that underwent different stresses during the 2022 season.

Supplementary Figure S7. Osmotic potential (π_0) measured in 2023 of *V. vinifera* cv. "Sauvignon blanc" that underwent different stresses during the 2022 season.

Supplementary Table S1. Comparative analysis of maximum transpiration (E_{max}) in control and esca-symptomatic *V. vinifera* cv. "Sauvignon blanc" during each week of drought stress.

Supplementary Table S2. Comparative analysis of predawn water potential (ψ_{PD}) in control and asymptomatic *V. vinifera* cv. "Sauvignon blanc" leaves during each week of drought stress.

Supplementary Table S3. Comparative analysis of stomatal conductance (g_s) and maximum Net CO_2 leaf assimilation (A_{max}) in control ("C"), asymptomatic ("AS") and esca-symptomatic ("S") *V. vinifera* cv. "Sauvignon blanc" leaves during each week of drought stress.

Funding

This work was supported by the program "Plan National Dépérissement du Vignoble" funded by FranceAgriMer and the Comité National des Interprofessions des Vins à appellation d'origine et à indication géographique (project ESCAPADE, 22001436), the Nouvelle-Aquitaine region (project VITIPIN, 22001439), and received financial support from the French government in the framework of the IdEX Bordeaux University "Investments for the Future" program/GPR Bordeaux Plant Sciences. Finally, G.S. was supported by a Chateaubriand grant from the French government.

Conflict of interest statement. None declared.

Data availability

Raw ecophysiological databases are available from the corresponding author upon reasonable request.

References

Andreini L, Caruso G, Bertolla C, Scalabrelli G, Viti R, Gucci R. Gas exchange, stem water potential and xylem flux on some grapevine cultivars affected by esca disease. *S Afr J Enol Vitic*. 2009:30(2):142–147. https://doi.org/10.21548/30-2-1434

Barigah TS, Bonhomme M, Lopez D, Traore A, Douris M, Venisse J-S, Cochard H, Badel E. Modulation of bud survival in Populus nigra sprouts in response to water stress-induced embolism. *Tree Physiol*. 2013:33(3):261–274. https://doi.org/10.1093/treephys/tpt002

Bartlett MK, Scoffoni C, Sack L. The determinants of leaf turgor loss point and prediction of drought tolerance of species and biomes: a global meta-analysis. *Ecol Lett*. 2012:15(5):393–405. https://doi.org/10.1111/j.1461-0248.2012.01751.x

Billon LM, Blackman CJ, Cochard H, Badel E, Hitmi A, Cartailler J, Souchal R, Torres-Ruiz JM. The DroughtBox: a new tool for phenotyping residual branch conductance and its temperature dependence during drought. *Plant Cell Environ*. 2020:43(6):1584–1594. https://doi.org/10.1111/pce.13750

Bortolami G, Farolfi E, Badel E, Burlett R, Cochard H, Ferrer N, King A, Lamarque LJ, Lecomte P, Marchesseau-Marchal M, *et al*. Seasonal and long-term consequences of esca grapevine disease on stem xylem integrity. *J Exp Bot*. 2021a:72(10):3914–3928. https://doi.org/10.1093/jxb/erab117

Bortolami G, Ferrer N, Baumgartner K, Delzon S, Gramaje D, Lamarque LJ, Romanazzi G, Gambetta GA, Delmas CEL. Esca grapevine disease involves leaf hydraulic failure and represents a unique premature senescence process. *Tree Physiol*. 2023:43(3):441–451. https://doi.org/10.1093/treephys/tpac133

Bortolami G, Gambetta GA, Cassan C, Dayer S, Farolfi E, Ferrer N, Gibon Y, Jolivet J, Lecomte P, Delmas CEL. Grapevines under drought do not express esca leaf symptoms. *Proc Natl Acad Sci U S A*. 2021b:118(43):e2112825118. https://doi.org/10.1073/pnas.2112825118

Bortolami G, Gambetta GA, Delzon S, Lamarque LJ, Pouzoulet J, Badel E, Burlett R, Charrier G, Cochard H, Dayer S, *et al*. Exploring the hydraulic failure hypothesis of esca leaf symptom formation. *Plant Physiol*. 2019:181(3):1163–1174. https://doi.org/10.1104/pp.19.00591

Brodribb TJ, Cochard H. Hydraulic failure defines the recovery and point of death in water-stressed conifers. *Plant Physiol*. 2009:149(1):575–584. https://doi.org/10.1104/pp.108.129783

Cao FY, Yoshioka K, Desveaux D. The roles of ABA in plant–pathogen interactions. *J Plant Res*. 2011:124(4):489–499. https://doi.org/10.1007/s10265-011-0409-y

Chaloner TM, Gurr SJ, Bebber DP. Plant pathogen infection risk tracks global crop yields under climate change. *Nat Clim Chang*. 2021:11(8):710–715. https://doi.org/10.1038/s41558-021-01104-8

Chanclud E, Morel J-B. Plant hormones: a fungal point of view. *Mol Plant Pathol*. 2016:17(8):1289–1297. https://doi.org/10.1111/mpp.12393

Charrier G. Extrapolating physiological response to drought through step-by-step analysis of water potential. *Plant Physiol*. 2020:184(2): 560–561. https://doi.org/10.1104/pp.20.01110

Charrier G, Delzon S, Domec J-C, Zhang L, Delmas CEL, Merlin I, Corso D, King A, Ojeda H, Ollat N, *et al*. Drought will not leave your glass empty: low risk of hydraulic failure revealed by long-term drought observations in world's top wine regions. *Sci Adv*. 2018:4(1):eaao6969. https://doi.org/10.1126/sciadv.aao6969

Choat B, Jansen S, Brodribb TJ, Cochard H, Delzon S, Bhaskar R, Bucci SJ, Feild TS, Gleason SM, Hacke UG, *et al*. Global convergence in the vulnerability of forests to drought. *Nature*. 2012:491(7426): 752–755. https://doi.org/10.1038/nature11688

Choat B, Lahr EC, Melcher PJ, Zwieniecki MA, Holbrook NM. The spatial pattern of air seeding thresholds in mature sugar maple trees. *Plant Cell Environ*. 2005:28(9):1082–1089. https://doi.org/10.1111/j.1365-3040.2005.01336.x

Cochard H, Tyree MT. Xylem dysfunction in Quercus: vessel sizes, tyloses, cavitation and seasonal changes in embolism. *Tree Physiol*. 1990:6(4):393–407. https://doi.org/10.1093/treephys/6.4.393

Davison EM, Tay FCS. The effect of waterlogging on seedlings of *Eucalyptus marginata*. *New Phytol*. 1985:101(4):743–753. https://doi.org/10.1111/j.1469-8137.1985.tb02879.x

Dayer S, Herrera JC, Dai Z, Burlett R, Lamarque LJ, Delzon S, Bortolami G, Cochard H, Gambetta GA. The sequence and thresholds of leaf hydraulic traits underlying grapevine varietal differences in drought tolerance. *J Exp Bot*. 2020:71(14):4333–4344. https://doi.org/10.1093/jxb/eraa186

Dell'Acqua N, Gambetta GA, Comont G, Ferrer N, Rochepeau A, Petriacq P, Delmas CEL. Nitrogen nutrition impacts grapevine esca leaf symptom incidence, physiology, and metabolism. *J Exp Bot*. 2025:76(11):3225–3242. https://doi.org/10.1093/jxb/eraf172

Dell'Acqua N, Gambetta GA, Delzon S, Ferrer N, Lamarque LJ, Saurin N, Theodore P, Delmas CEL. Mechanisms of grapevine resilience to a vascular disease: investigating stem radial growth, xylem development and physiological acclimation. *Ann Bot*. 2024:133(2): 321–336. https://doi.org/10.1093/aob/mcad188

De Micco V, Balzano A, Wheeler EA, Baas P. Tyloses and gums: a review of structure, function and occurrence of vessel occlusions. *IAWA J*. 2016:37(2):186–205. https://doi.org/10.1163/22941932-20160130

Desprez-Loustau M-L, Marçais B, Nageleisen L-M, Piou D, Vannini A. Interactive effects of drought and pathogens in forest trees. *Ann For Sci*. 2006:63(6):597–612. https://doi.org/10.1051/forest:2006040

Edwards J, Salib S, Thomson F, Pascoe IG. The impact of *Phaeomoniella chlamydospora* infection on the grapevine's physiological response to water stress part 1: zinfandel. *Phytopathol Mediterr*. 2007a:46(1): 26–37. https://doi.org/10.14601/Phytopathol_Mediterr-1855

Edwards J, Salib S, Thomson F, Pascoe IG. The impact of *Phaeomoniella chlamydospora* infection on the grapevine's physiological response to water stress part 2: cabernet sauvignon and chardonnay. *Phytopathol Mediterr*. 2007b:46:38–49. https://doi.org/10.14601/Phytopathol_Mediterr-1856

Fanton AC, Brodersen C. Hydraulic consequences of enzymatic breakdown of grapevine pit membranes. *Plant Physiol*. 2021:186(4): 1919–1931. https://doi.org/10.1093/plphys/kiab191

Fischer M, Peighami Ashnaei S. Grapevine, esca complex, and environment: the disease triangle. *Phytopathol Mediterr*. 2019:58: 17–37. https://doi.org/10.14601/Phytopathol_Mediterr-25086

Fontaine F, Pinto C, Vallet J, Clement C, Gomes AC, Spagnolo A. The effects of grapevine trunk diseases (GTDs) on vine physiology. *Eur J Plant Pathol*. 2016:144(4):707–721. https://doi.org/10.1007/s10658-015-0770-0

Fujita M, Fujita Y, Noutoshi Y, Takahashi F, Narusaka Y, Yamaguchi-Shinozaki K. Crosstalk between abiotic and biotic stress responses: a current view from the points of convergence in the stress signaling networks. *Curr Opin Plant Biol*. 2006:9(4):436–442. https://doi.org/10.1016/j.pbi.2006.05.014

Gambetta GA, Herrera JC, Dayer S, Feng Q, Hochberg U, Castellarin SD. The physiology of drought stress in grapevine: towards an integrative definition of drought tolerance. *J Exp Bot*. 2020:71(16): 4658–4676. https://doi.org/10.1093/jxb/eraa245

Gärtner H, Lucchinetti S, Schweingruber FH. New perspectives for wood anatomical analysis in dendrosciences: the GSL1-microtome. *Dendrochronologia*. 2014:32(1):47–51. https://doi.org/10.1016/j.dendro.2013.07.002

Gauthey A, Peters JMR, Lòpez R, Carins-Murphy MR, Rodriguez-Dominguez CM, Tissue DT, Medlyn BE, Brodribb TJ, Choat B. Mechanisms of xylem hydraulic recovery after drought in *Eucalyptus saligna*. *Plant Cell Environ*. 2022:45(4):1216–1228. https://doi.org/10.1111/pce.14265

Gramaje D, Armengol J. Fungal trunk pathogens in the grapevine propagation process: potential inoculum sources, detection, identification, and management strategies. *Plant Dis*. 2011:95(9): 1040–1055. https://doi.org/10.1094/PDIS-01-11-0025

Gupta A, Rico-Medina A, Caño-Delgado AI. The physiology of plant responses to drought. *Science*. 2020:368(6488):266–269. https://doi.org/10.1126/science.aaz7614

Herrera JC, Savoi S, Dostal J, Elezovic K, Chatzisavva M, Forneck A, Savi T. The legacy of past droughts induces water-sparingly behaviour in Grüner Veltliner grapevines. *Plant Biol J*. 2024. https://doi.org/10.1111/plb.13620

Hochberg U, Bonel AG, David-Schwartz R, Degu A, Fait A, Cochard H, Peterlunger E, Herrera JC. Grapevine acclimation to water deficit: the adjustment of stomatal and hydraulic conductance differs from petiole embolism vulnerability. *Planta*. 2017:245(6): 1091–1104. https://doi.org/10.1007/s00425-017-2662-3

Hochberg U, Perry A, Rachmilevitch S, Ben-Gal A, Sperling O. Instantaneous and lasting effects of drought on grapevine water use. *Agric For Meteorol*. 2023:338:109521. https://doi.org/10.1016/j.agrformet.2023.109521

Hossain M, Veneklaas EJ, Hardy GESJ, Poot P. Tree host–pathogen interactions as influenced by drought timing: linking physiological performance, biochemical defence and disease severity. *Tree Physiol*. 2019:39(1):6–18. https://doi.org/10.1093/treephys/tpy113

Knipfer T, Bambach N, Hernandez MI, Bartlett MK, Sinclair G, Duong F, Kluepfel DA, McElrone AJ. Predicting stomatal closure and turgor loss in woody plants using predawn and midday water potential. *Plant Physiol*. 2020:184(2):881–894. https://doi.org/10.1104/pp.20.00500

Lamacque L, Charrier G, Farnese FDS, Lemaire B, Améglio T, Herbette S. Drought-induced mortality: stem diameter variation reveals a point of no return in lavender species. *Plant Physiol*. 2020:183(4):1638–1649. https://doi.org/10.1104/pp.20.00165.

Lamarque LJ, Delmas CEL, Charrier G, Burlett R, Dell'Acqua N, Pouzoulet J, Gambetta GA, Delzon S. Quantifying the grapevine xylem embolism resistance spectrum to identify varieties and regions at risk in a future dry climate. *Sci Rep*. 2023:13(1):7724. https://doi.org/10.1038/s41598-023-34224-6

Lecomte P, Bénétreau C, Diarra B, Meziani Y, Delmas C, Fermaud M. Logistic modeling of summer expression of esca symptoms in tolerant and susceptible cultivars in bordeaux vineyards. *OENO One*. 2024:58(1). https://doi.org/10.20870/oeno-one.2024.58.1.7571

Lecomte P, Darrieutort G, Liminana J-M, Comont G, Muruamendiaraz A, Legorburu F-J, Choueiri E, Jreijiri F, El Amil R, Fermaud M. New insights into esca of grapevine: the development of foliar

symptoms and their association with xylem discoloration. *Plant Dis*. 2012:96(7):924–934. https://doi.org/10.1094/PDIS-09-11-0776-RE

Le Menn N, van Leeuwen C, Picard M, Riquier L, de Revel G, Marchand S. Effect of vine water and nitrogen status, as well as temperature, on some aroma compounds of aged red Bordeaux wines. *J Agric Food Chem*. 2019:67(25):7098–7109. https://doi.org/10.1021/acs.jafc.9b00591

Maher N, Piot J, Bastien S, Vallance J, Rey P, Guérin-Dubrana L. Wood necrosis in esca-affected vines: types, relationships and possible links with foliar symptom expression. *OENO One*. 2012:46(1):15. https://doi.org/10.20870/oeno-one.2012.46.1.1507

Martínez-Vilalta J, Poyatos R, Aguadé D, Retana J, Mencuccini M. A new look at water transport regulation in plants. *New Phytol*. 2014:204(1):105–115. https://doi.org/10.1111/nph.12912

McDowell N, Pockman WT, Allen CD, Breshears DD, Cobb N, Kolb T, Plaut J, Sperry J, West A, Williams DG, *et al*. Mechanisms of plant survival and mortality during drought: why do some plants survive while others succumb to drought? *New Phytol*. 2008:178(4):719–739. https://doi.org/10.1111/j.1469-8137.2008.02436.x

Mondello V, Larignon P, Armengol J, Kortekamp A, Vaczy K, Prezman F, Serrano E, Rego C, Mugnai L, Fontaine F. Management of grapevine trunk diseases: knowledge transfer, current strategies and innovative strategies adopted in Europe. *Phytopathol Mediterr*. 2018:57:369–383. https://doi.org/10.14601/Phytopathol_Mediterr-23942

Mugnai L, Graniti A, Surico G. Esca (black measles) and brown wood-streaking: two old and elusive diseases of grapevines. *Plant Dis*. 1999:83(5):404–418. https://doi.org/10.1094/PDIS.1999.83.5.404

Niinemets Ü. Responses of forest trees to single and multiple environmental stresses from seedlings to mature plants: past stress history, stress interactions, tolerance and acclimation. *For Ecol Manage*. 2010:260(10):1623–1639. https://doi.org/10.1016/j.foreco.2010.07.054

Oliva J, Stenlid J, Martínez-Vilalta J. The effect of fungal pathogens on the water and carbon economy of trees: implications for drought-induced mortality. *New Phytol*. 2014:203(4):1028–1035. https://doi.org/10.1111/nph.12857

Ouadi L, Bruez E, Bastien S, Vallance J, Lecomte P, Domec J-C, Rey P. Ecophysiological impacts of esca, a devastating grapevine trunk disease, on Vitis vinifera L. *PLoS One*. 2019:14(9):e0222586. https://doi.org/10.1371/journal.pone.0222586

Petit A-N, Vaillant N, Boulay M, Clément C, Fontaine F. Alteration of photosynthesis in grapevines affected by esca. *Phytopathology*. 2006:96(10):1060–1066. https://doi.org/10.1094/PHYTO-96-1060

Ramegowda V, Senthil-Kumar M. The interactive effects of simultaneous biotic and abiotic stresses on plants: mechanistic understanding from drought and pathogen combination. *J Plant Physiol*. 2015:176:47–54. https://doi.org/10.1016/j.jplph.2014.11.008

Singh BK, Delgado-Baquerizo M, Egidi E, Guirado E, Leach JE, Liu H, Trivedi P. Climate change impacts on plant pathogens, food security and paths forward. *Nat Rev Microbiol*. 2023:21(10):640–656. https://doi.org/10.1038/s41579-023-00900-7

Spiegel-Roy P. Domestication of fruit trees. In: Barigozzi C, editor. *Developments in agricultural and managed forest ecology*. Netherlands: Elsevier; 1986. p. 201–211.

Sun Q, Rost TL, Reid MS, Matthews MA. Ethylene and not embolism is required for wound-induced tylose development in stems of grapevines. *Plant Physiol*. 2007:145(4):1629–1636. https://doi.org/10.1104/pp.107.100537

Tombesi S, Frioni T, Poni S, Palliotti A. Effect of water stress "memory" on plant behavior during subsequent drought stress. *Environ Exp Bot*. 2018:150:106–114. https://doi.org/10.1016/j.envexpbot.2018.03.009

Torres-Ruiz JM, Cochard H, Delzon S, Boivin T, Burlett R, Cailleret M, Corso D, Delmas CEL, De Caceres M, Diaz-Espejo A, *et al*. Plant hydraulics at the heart of plant, crops and ecosystem functions in the face of climate change. *New Phytol*. 2024:241(3):984–999. https://doi.org/10.1111/nph.19463

Triolo R, Roby JP, Pisciotta A, Di Lorenzo R, van Leeuwen C. Impact of vine water status on berry mass and berry tissue development of Cabernet franc (*Vitis vinifera L.*), assessed at berry level. *J Sci Food Agric*. 2019:99(13):5711–5719. https://doi.org/10.1002/jsfa.9834

Trumbore S, Brando P, Hartmann H. Forest health and global change. *Science*. 2015:349(6250):814–818. https://doi.org/10.1126/science.aac6759

Tyree M, Ewers F. The hydraulic architecture of trees and other woody-plants. *New Phytol*. 1991:119(3):345–360. https://doi.org/10.1111/j.1469-8137.1991.tb00035.x

Wilcox KR, von Fischer JC, Muscha JM, Petersen MK, Knapp AK. Contrasting above- and belowground sensitivity of three great plains grasslands to altered rainfall regimes. *Glob Chang Biol*. 2015:21(1):335–344. https://doi.org/10.1111/gcb.12673

Xu P, Chen F, Mannas JP, Feldman T, Sumner LW, Roossinck MJ. Virus infection improves drought tolerance. *New Phytol*. 2008:180(4):911–921. https://doi.org/10.1111/j.1469-8137.2008.02627.x

Zweifel R, Item H, Häsler R. Link between diurnal stem radius changes and tree water relations. *Tree Physiol*. 2001:21(12–13):869–877. https://doi.org/10.1093/treephys/21.12-13.869